Available online at www.sciencedirect.com
ScienceDirect
Ceramics International 36 (2010) 1417–1422
CERAMICS INTERNATIONAL
www.elsevier.com/locate/ceramint

Hydrothermal synthesis of magnetite nanoparticles as MRI contrast agents

C.Y. Haw [a], F. Mohamed [a], C.H. Chia [a,*], S. Radiman [a], S. Zakaria [a], N.M. Huang [b], H.N. Lim [c]

[a] School of Applied Physics, Faculty of Science and Technology, Universiti Kebangsaan Malaysia, 43600 Bangi, Selangor, Malaysia
[b] Solid State Physics Research Laboratory, Physics Department, University of Malaya, 50603 Kuala Lumpur, Malaysia
[c] Chemistry Department, Faculty of Science, Universiti Putra Malaysia, 43400 UPM Serdang, Selangor, Malaysia

Received 14 December 2009; received in revised form 22 December 2009; accepted 30 January 2010
Available online 1 March 2010

Abstract

Magnetite (Fe_3O_4) nanoparticles prepared using hydrothermal approach were employed to study their potential application as magnetic resonance imaging (MRI) contrast agent. The hydrothermal process involves precursors $FeCl_2{\cdot}4H_2O$ and $FeCl_3$ with NaOH as reducing agent to initiate the precipitation of Fe_3O_4, followed by hydrothermal treatment to produce nano-sized Fe_3O_4. Chitosan (CTS) was coated onto the surface of the as-prepared Fe_3O_4 nanoparticles to enhance its stability and biocompatible properties. The size distribution of the obtained Fe_3O_4 nanoparticles was examined using transmission electron microscopy (TEM). The cubic inverse spinel structure of Fe_3O_4 nanoparticles was confirmed by X-ray diffraction technique (XRD). Fourier transform infrared (FTIR) spectrum indicated the presence of the chitosan on the surface of the Fe_3O_4 nanoparticles. The superparamagnetic behaviour of the produced Fe_3O_4 nanoparticles at room temperature was elucidated using a vibrating sample magnetometer (VSM). From the result of custom made phantom study of magnetic resonance (MR) imaging, coated Fe_3O_4 nanoparticles have been proved to be a promising contrast enhanced agent in MR imaging.

Keywords: B. Surfaces; C. Magnetic properties; E. Biomedical applications; Hydrothermal

1. Introduction

A plethora of researches on Fe_3O_4 nanoparticles have been carried out worldwide nowadays. This is attributed to its broad range of applications especially in biomedical applications such as cellular therapy in cell labelling [1,2], targeted drug delivery [3], selective protein separation [4,5], MRI contrast agent [6,7] and hyperthermia in cancer treatment [8,9].

All these therapeutic approaches require Fe_3O_4 nanoparticles with narrow size distribution, superparamagnetic behaviour and specific surface modification. There are two main reasons of surface modification, i.e., to increase the properties of biocompatibility and to avoid the agglomeration of the naked particles due to the magnetostatic interaction [10]. Chitosan is one of the consensual biocompatible, biodegradable and non-toxic natural linear polyaminosaccharides. Therefore, it is suitable to be used as surface-modification material to improve the compatibility of the nanoparticles in aqueous medium of human body [11].

In this study, hydrothermal method was chosen to produce Fe_3O_4 nanoparticles due to its advantages: the use of organic reagents are waived, relatively cost-effective, high yield of products and excellent particle crystallinity with controllable size and good morphology of particles can be easily obtained. In addition, no post-heat treatment is required for the produced nanoparticles which makes this method highly desirable as heat treatment might result in particle agglomeration [12].

In the present investigation, our goal is to prepare chitosan-functionalized superparamagnetic Fe_3O_4 nanoparticles and to study its potential application as MRI contrast agent. The as-prepared Fe_3O_4 nanoparticles were characterized with various instruments such as transmission electron microscopy (TEM), X-ray diffraction (XRD), vibrating sample magnetometer (VSM) and Fourier transform infrared spectroscopy (FTIR). In addition, the particles contrast enhancement property was evaluated using custom made Perspex phantom in the T_2-weighted study of MRI.

* Corresponding author. Tel.: +60 3 89215473; fax: +60 3 89213777.
E-mail address: chia@ukm.my (C.H. Chia).

0272-8842/$36.00
doi:10.1016/j.ceramint.2010.02.005

2. Experimental

2.1. Materials

The chemicals used were analytical grade. Ferrous sulphate heptahydrate ($FeSO_4{\cdot}7H_2O$), ferric chloride ($FeCl_3$), hydrochloride acid (HCl) (Fischer Chemicals Ltd.), sodium hydroxide (NaOH) and ethanol (99.9%, Merck KgaA) were used for the preparation of Fe_3O_4 nanoparticles. On the other hand, the surface functionalization process of Fe_3O_4 requires medium molecular weight chitosan (Kasei Kogyo Co. Ltd., Tokyo), paraffin (LabChem), SPAN-80 (OHG, Merck Schuchardt), acetic acid (R & M Chemicals) and glutaraldehyde (25%, Unilab) as binder. The water used in all experiments was deionised water filtered by Purelab Maxima ELGA and the resistivity of water was 18.2 MΩ.

2.2. Methods

The synthesis process can be divided into four steps, i.e., preparation of Fe_3O_4 nanoparticles, surface functionalization of Fe_3O_4 with chitosan, characterization of Fe_3O_4 nanoparticles and MRI contrast study.

2.2.1. Synthesis of superparamagnetic Fe_3O_4 nanoparticles

The synthesis of Fe_3O_4 nanoparticles (Fe_3O_4 nanoparticles) was carried out by precipitating $FeSO_4{\cdot}7H_2O$ and $FeCl_3$ in alkaline medium (NaOH) with a molar ratio of Fe^{2+}:Fe^{3+}:OH^- at 1:2:8. Prior to this step, 0.01 M of HCl was diluted by using deionised water (DIW) and used for the whole process of the preparation of Fe_3O_4 nanoparticles. This procedure was important to avoid the precipitation of other iron oxides before the addition of alkaline. The mixture was added into a N_2 blanketed three neck flask and the stirring was kept at constant rate for 5 min. After that, the precipitated black product was immediately added into a Teflon-lined stainless steel autoclave with 60 ml capacity. The autoclave was subsequently placed in a furnace at 200 °C for 1 h. The autoclave was cooled naturally after the hydrothermal treatment and the precipitate was recovered and followed by washing with DIW and ethanol for 3 times to eliminate any unwanted impurities. Finally, the collected black Fe_3O_4 nanoparticles were dried in an oven at 45 °C for 24 h.

2.2.2. Surface coating of Fe_3O_4 nanoparticles with chitosan

Chitosan solution was prepared by mixing 99.0 ml acetic acid solution (2%) with 1.0 g of chitosan. The mixture was stirred for 48 h using magnetic stirrer with constant speed to ensure the chitosan swelled completely. Essentially, 0.5 g of as-prepared Fe_3O_4 nanoparticles was dispersed in a solution with 30 ml paraffin and 0.5 ml SPAN-80. The above mixture was added with 2 ml of chitosan solution and stirred vigorously for 40 min. The functionalization of chitosan on Fe_3O_4 nanoparticles can be aided via the addition of 3 ml of glutaraldehyde into the mixture. The mixture was vigorously stirred for another 3 h. A dark brown precipitate will be obtained and then washed with ethanol and distilled water for 3 times to remove excessive chitosan and other chemicals. The final product was subsequently dried at 50 °C overnight.

2.2.3. Characterization of Fe_3O_4 nanoparticles and chitosan–Fe_3O_4 nanoparticles

Transmission electron microscopy (TEM): the average particle diameter, size distribution and morphology of Fe_3O_4 nanoparticles were studied using a Philips CM-12 transmission electron microscope operating at an accelerating voltage of 100 kV. A drop of the sample was placed onto the carbon-coated copper grids and the solvent was left to dry off at room temperature before examination.

X-ray diffraction measurement (XRD): X-ray diffraction (XRD) technique is an effective tool to ascertain crystal structure of Fe_3O_4 nanoparticles. Cu K_α radiation was used to investigate purity of Fe_3O_4 powder in the range of 2θ from 20° to 80°. The crystal structure of Fe_3O_4 nanoparticles was confirmed using a Siemens D-5000. Typically, 0.1 g of lean sample (use pure Fe_3O_4 viz. without particles coating) was used for the XRD scanning with an unfiltered Cu K_α radiation. The spectrum obtained was therefore compared with the standard peaks provided by *JCDPS 00-019-0629 of International Center for Diffraction Data*.

Vibrating samples magnetometer (VSM): the magnetic properties of synthesized Fe_3O_4 nanoparticles were measured by a LakeShore 736 vibrating sample magnetometer operating at 298 K. The samples were vibrated at a frequency of 85 Hz to shear the magnetic flux created and any signal generated from the samples was recorded by a Gauss meter.

Fourier transform infrared (FTIR): the adsorption of certain functional groups on the Fe_3O_4 nanoparticles surface as a result of chitosan coating process can be determined with a FTIR Perkin Elmer GX. The coated sample was first treated with KBr method and was examined in the range of wavelength number of 370–4000 cm^{-1}.

2.2.4. MRI contrast study

Prior to the MR scanning, a custom made Perspex phantom was prepared using Perspex petri dish (refer Fig. 1). Essentially,

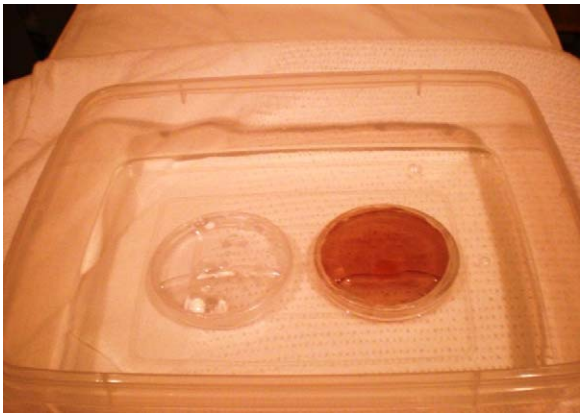

Fig. 1. Custom made MRI phantoms both contain phosphate buffer solution, with monodisperse ferrofluid (on the right) and a control (on the left) without ferrofluid.

ferrofluid was prepared by using 0.5 mg of the chitosan–Fe_3O_4 nanoparticles and mixed thoroughly with phosphate buffer solution (PBS, pH 7.4). Later, the ferrofluid was transferred into the Perspex phantom and sealed tightly with parafilm. Another phantom which consists of DIW only was prepared as control and both of the phantoms were placed inside a plastic box that was filled with water previously. The MR imaging measurements were carried out on a Siemens Symphony Medical System with magnetic field intensity of 1.5 T. The as-prepared phantoms were placed stagnantly with a Perspex holder positioned in an isocentre of the MR machine. A volume coil was served as a signal relay for both transmission of radio frequency (RF) pulses and signal reception. The parameters used for the examination were field of view (FOV) = 250 mm × 250 mm, slice thickness = 1.0 mm for 13 slices, echo time (TE) = 76 ms and relaxation time (TR) = 3600 ms for both phantoms. The MR image was later analyzed based on the contrast quality of both phantoms to determine qualitatively the potential use of synthesized Fe_3O_4 nanoparticles as contrast agent of MRI.

3. Results and discussion

The formation of Fe_3O_4 nanoparticles can be explained by two steps, i.e., precipitation of Fe_3O_4 nanoparticles and hydrothermal treatment. The chemical reaction of the precipitation of Fe_3O_4 at the first stage can be expressed as below:

$$Fe^{2+} + 2Fe^{3+} + 8OH^- \rightarrow Fe_3O_4 + 4H_2O \quad (1)$$

where Fe_3O_4 representing the combination of divalent and trivalent iron atoms. Wei and Viadero suggested that the molar ratio between Fe^{2+} and Fe^{3+} should be maintained at 1:2 in order to obtain high quality Fe_3O_4 [13]. In our study, the molar ratio of Fe^{2+}:Fe^{3+} was kept at 1:2 in a deoxygenated condition. This is to ensure that high purity Fe_3O_4 phase can be obtained without the presence of any other iron oxide phases, such as goethite and hematite [14]. Based on our observation, brownish precipitation can be observed during the mixing of Fe^{2+} and Fe^{3+} under vigorous stirring, followed by a very viscous black precipitation once NaOH is added into the mixture. The black precipitate is deduced as the premature product of oxidized mixture of reactants of Fe^{2+} and Fe^{3+} which consisted of interphase of FeO(OH) crystal or ferric oxyhydroxides, as proposed by our previous study [15]. The black precipitate is then transferred into an autoclave and heated to 200 °C for 1 h. Hydrothermal treatment provides good revenue as the supercritical condition which enhances the dissolution of thermodynamically unstable iron oxyhydroxides. Furthermore, the high heat energy and pressure in the autoclave facilitates fracture of the Fe_3O_4 macronucleus to form nano-sized particles. In this respect, the temperature used in this study (200 °C) will accelerate the dissolution of Fe_3O_4 macronucleus and subsequently generate nanoscale Fe_3O_4 particles. Earlier studies suggest that if hydrothermal temperature is greater than 160 °C, it would possibly result in bigger particles size. Lower hydrothermal temperatures of 120 or 80 °C have a tendency to produce smaller size distribution of Fe_3O_4 nanoparticles [16,17]. Besides, the duration of heating process may also play important role in the production of Fe_3O_4 nanoparticles. Mao et al. synthesized Fe_3O_4 nanoparticles at 180 °C for 24 h and their results indicate that the Fe_3O_4 nanoparticles produced are of well-defined crystal shape and bigger due to the recrystallization [18]. Contrastingly, in this study, the obtained Fe_3O_4 nanoparticles are of spherical shape with average diameters of 17.12 nm (Fig. 2). From the TEM micrograph, we notice that the Fe_3O_4 nanoparticles are attached to one another which may due to the high surface energy of the nanoparticles. Kim et al. suggest that the existence of the van der Waals interaction between the particles has resulted in the aggregation of the particles [19]. Maity and Agrawal, however, report that the aggregation of the Fe_3O_4 nanoparticles is essentially due to magnetostatic interaction as a result of the dipole–dipole interaction [10].

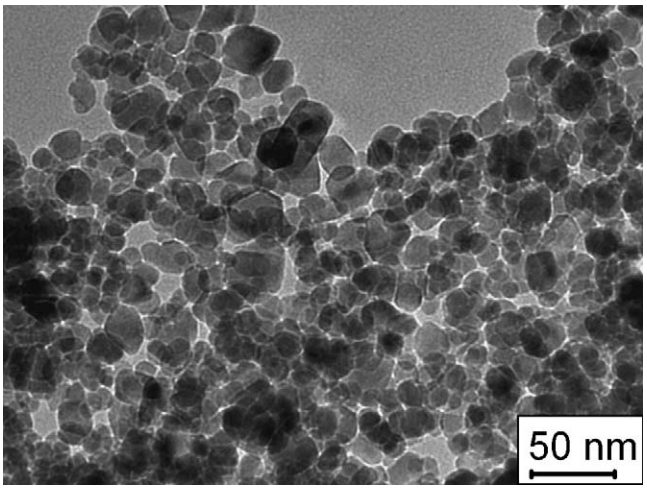

Fig. 2. TEM micrograph for Fe_3O_4 nanoparticles synthesized through hydrothermal method at 200 °C for 1 h.

Fig. 3 shows the size distribution of the Fe_3O_4 nanoparticles synthesized using hydrothermal method. The result is obtained by measuring at least 200 particles from TEM micrographs. The average diameter of the obtained Fe_3O_4 nanoparticles is

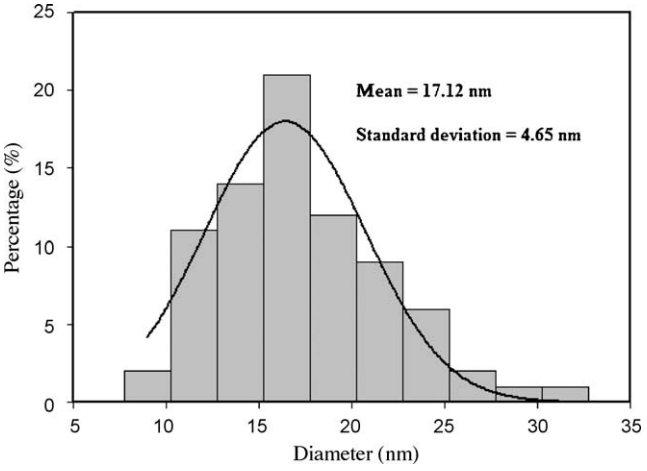

Fig. 3. Histogram of the size distribution of Fe_3O_4 nanoparticles. The size distribution of particles is seemingly shift to the left indicates smaller size of particles have been produced.

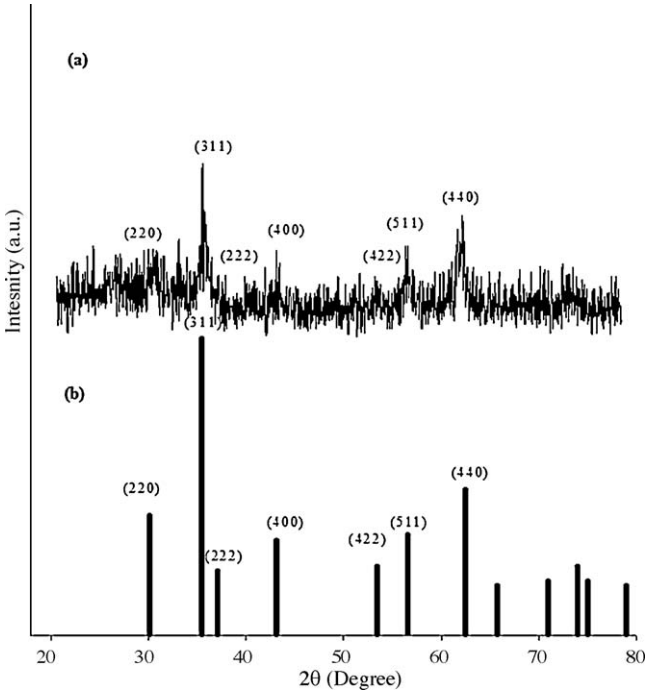

Fig. 4. XRD spectra for (a) synthesized Fe_3O_4 nanoparticles; (b) standard reference (JCPDS: 19-0629).

17.12 ± 4.65 nm. It indicates that the nanoparticles produced using hydrothermal method possesses narrow distribution.

The XRD pattern of Fe_3O_4 nanoparticles samples is presented in Fig. 4. All the characteristic peaks are consistent with the standard database peaks, revealing the cubic inverse spinel structure of the sample. The 2θ peaks with significant intensity at 30.20°, 35.44°, 37.12°, 43.36°, 53.80°, 57.04° and 62.43°, respectively, were in accordance with the $d_{h\,k\,l}$ crystal planes of Fe_3O_4 at (2 2 0), (3 1 1), (2 2 2), (4 0 0), (4 2 2), (5 1 1), and (4 4 0), which agree well with the standard peak values of XRD pattern of Fe_3O_4 (JCPDS: 19-0629). The successful formation of Fe_3O_4 nanoparticles can further be confirmed from the dark color of the resulting products.

The magnetization of the obtained Fe_3O_4 nanoparticles is shown in Fig. 5. As can be seen that the saturation magnetization (M_s) of the sample is 57.40 emu/g. The reduction

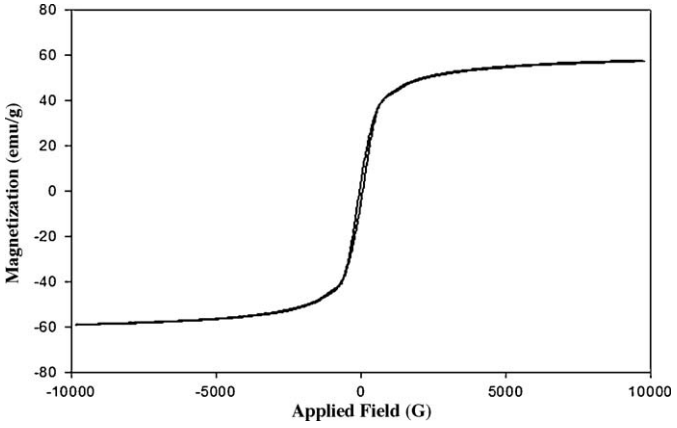

Fig. 5. Hysteresis loop obtained for Fe_3O_4 nanoparticles measured at 298 K.

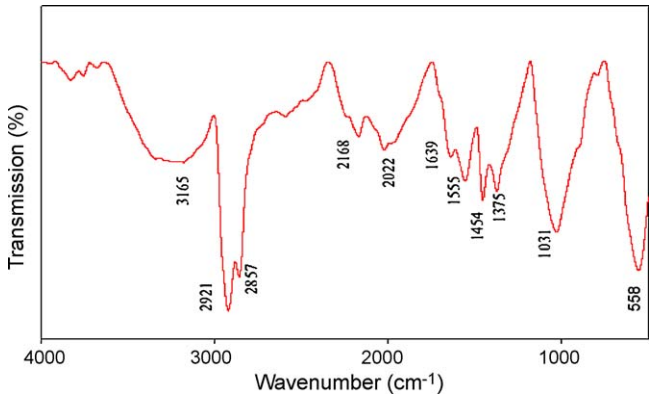

Fig. 6. FTIR spectrum for chitosan coated Fe_3O_4 nanoparticles.

of the saturation magnetization compared to that of bulk Fe_3O_4 (~92 emu/g) could be explained by the finite size and surface disorder of the produced Fe_3O_4 nanoparticles [20]. Nedkov et al. has also reported that the surface deformation, cation distribution and Laplace pressure might reduced the value of M_s of the Fe_3O_4 nanoparticles [21]. The result also reveals the superparamagnetic behaviour of the produced Fe_3O_4 nanoparticles due to its relatively low remanence magnetization and the coercivity.

Fig. 6 presents the IR spectrum of the as-prepared chitosan–Fe_3O_4 nanoparticles. In this study, chitosan has been chosen as surface modifier through the reverse cross-linking with the addition of glutaraldehyde acts as binder. This binder is important in order to connect the network of long chains of chitosan to that of Fe_3O_4 surfaces. The adsorption peaks at around 558 cm^{-1} is observed in the spectrum which can be attributed to the adsorption of Fe–O bond [16,22]. Furthermore, three significant peaks can also be observed at 1031, 2022 and 2168 cm^{-1}, corresponding to the stretching of single bond of carbonyl group (C=O) from the chitosan molecules of its own [23]. There are two adsorption bands at ~1454 and 1375 cm^{-1}, corresponding to the non-symmetry of –CH stretching. On the other hand, the characteristic adsorption at 1639 and 1555 cm^{-1} is referred to the amide groups (CN) [24]. Comparably, our study has shown that the band of 1639 cm^{-1} in Fig. 6 is rather short. This can be deduced that some of the chitosan molecules have been cross-linked by glutaraldehyde which eventually reduces the transmission of the FTIR peak. Li et al. (2008) also suggest the formation of *Schiff* base after the introduction of glutaraldehyde [16]. In addition, two significant adsorption peaks are also observed in this spectrum, i.e., 2921 and 2857 cm^{-1}, which are associated with the –CH group [25]. The peak at ~2857 cm^{-1} was shorter and it is dominated by 2921 cm^{-1}. A short peak covering a broad band at 3165 cm^{-1} can be described as stretching of amine groups ($-NH_2$) of chitosan from some small amounts of residual of chitosan which are presumably not coated onto the surface of particle. This may attributed to the fact that certain chitosan molecules do not cross-linked by the glutaraldehyde which plays a bridging function to link between chitosan molecules and the naked Fe_3O_4 nanoparticles. This result is in agreement with previous finding and further support the fact

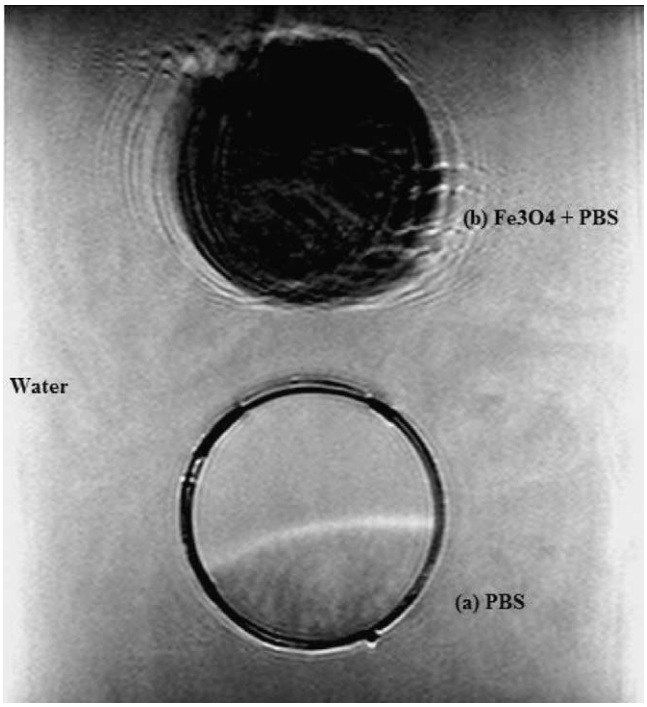

Fig. 7. MRI analysis image at T_2-weighted imaging showed 2 phantom cells (a) phosphate buffer solution only; and (b) with monodisperse ferrofluid in phosphate buffer solution (PBS).

that the Fe_3O_4 nanoparticles has been surface treated with chitosan molecules [16].

To investigate the chitosan–Fe_3O_4 nanoparticles potential application as MRI contrast agent, a custom made Perspex phantom was fabricated together with the administration of monodisperse ferrofluid and phosphate buffer solution (PBS). Two phantoms are prepared as one served as a control, i.e., contained PBS without the addition of ferrofluid and another one, however, contained chitosan–Fe_3O_4 nanoparticles ferrofluid. A T_2-weighted MR image acquires to compare the two phantoms and an image after MRI examination was given in Fig. 7. Apparently, Fig. 7(a) shows the quality of contrast of MRI image was drastically darkened whereas Fig. 7(b) shows no effect of contrast enhancement as the brightness is similar to the surrounding water. The water surrounded both phantom cells exhibited hyperintensity due to randomly oriented distribution of water molecules.

T_2-Weighted image obtained as a result from the relaxation of hydrogen atoms (spin–spin interaction) at transverse plane. T_2 is the time required for the proton dephase rapidly to 37% of the initial amplitude of the signal generated. The process occurred in a very short period of time and the relayed signal measured across the (x,y) plane in the magnetic moment of proton decreases with the time. T_2 for fatty tissue in the body has a shorter dephasing relatively compare to the water molecules. Hence, less signal will be detected and causing the image to be darkly appeared. In contrast, water molecule has longer dephase of time and signal received is much more better resulting the image to be brightly appeared at T_2-weighted analysis. This explained the reason for the T_2-weighted image as shown in Fig. 7(b).

Fig. 7(a), however, can be explained by the property of the particles itself. Jain et al. suggested that the relaxation of proton at T_2 happened due to some exchange of energy between the water molecules itself [7]. Superparamagnetic Fe_3O_4 nanoparticles do not retain magnetic moment (in general speaking not being magnetized) although the external magnetic field is removed provides a good property for the contrast enhancement in MRI scanning. This is attributed to the disarrangement of magnetic field of the particles and indirectly helps to shortening of T_2 time. Subsequently, reducing the brightness and the image will be darkly appeared as a result from decreasing of the signal detected. Hence, the contrast of the image can be enhanced by the introduction of superparamagnetic Fe_3O_4 nanoparticles. The MRI experimental results suggest that Fe_3O_4 nanoparticles synthesized by hydrothermal method could be potentially used as MRI contrast agent.

4. Conclusion

Hydrothermally synthesized superparamagnetic Fe_3O_4 nanoparticles have been employed as MRI contrast agent in the Perspex phantom to study the T_2-weighted MR image. TEM and XRD results indicate that the average size of particles was 17.22 nm in diameter and good crystallinity was preserved suggest that our particles are purely Fe_3O_4 nanoparticles. VSM result confirms that our particles possessed superparamagnetic property with saturated magnetization of 57.40 emu/g. The presence of chitosan functional groups has been confirmed through FTIR spectrum which shows that chitosan is coated onto the particles surface. The chitosan–Fe_3O_4 presents a bolstered enhancement of MR image contrast compared to the control phantom. Therefore, this shows that chitosan–Fe_3O_4 nanoparticles can be utilized as a promising contrast agent for MRI.

Acknowledgements

The work was financially supported by the Scientific Advancement Fund Allocation (STGL-009-2006) and ScienceFund (03-01-02-SF0030). The authors thank the staffs of the Microscope Unit of Universiti Kebangsaan Malaysia (UKM) for their assistance in obtaining the SEM and TEM images.

References

[1] J.C. Sipe, M. Filippi, G. Martino, R. Furlan, M.A. Rocca, M. Rovaris, A. Bergami, J. Zyroff, G. Scotti, G. Comi, Method for intracellular magnetic labeling of human mononuclear cells using approved iron contrast agents, Magnetic Resonance Imaging 17 (10) (1999) 1521–1523.

[2] E. Farrell, P. Wielopolskix, P. Pavljasevic, N. Kops, H. Weinans, M.R. Bernsenx, G.J.V.M. van Osch, Cell labelling with superparamagnetic iron oxide has no effect on chondrocyte behaviour, Osteoarthritis and Cartilage 17 (2009) 961–967.

[3] Y. Yoshida, S. Fukui, S. Fujimoto, F. Mishima, S. Takeda, Y. Izumi, S. Ohtani, Y. Fujitani, S. Nishijima, Ex vivo investigation of magnetically targeted drug delivery system, Journal of Magnetism and Magnetic Materials 310 (2) (2007) 2880–2882.

[4] S. Bucak, D.A. Jones, P.E. Laibinis, T.A. Hatton, Protein separations using colloidal magnetic nanoparticles, Biotechnology Progress 19 (2003) 477–484.

[5] B.H. Jun, M.S. Noh, G.S. Kim, H.M. Kang, J.H. Kim, W.J. Chung, M.S. Kim, Y.K. Kim, M.H. Cho, D.H. Jeong, Y.S. Lee, Protein separation and identification using magnetic beads encoded with surface-enhanced Raman spectroscopy, Analytical Biochemistry 391 (2009) 24–30.
[6] M. Corti, A. Lascialfari, G.S. Marinone, A. Masotti, E. Micotti, F. Orsini, G. Ortaggi, G. Poletti, C. Innocenti, C. Sangregorio, Magnetic and relaxometric properties of polyethylenimine-coated superparamagnetic MRI contrast agents, Journal of Magnetism and Magnetic Materials 320 (2008) 316–319.
[7] T.K. Jain, J. Richey, M. Strand, D.L. Leslie-Pelecky, C.A. Flask, V. Labhasetwar, Magnetic nanoparticles with dual functional properties: drug delivery and magnetic resonance imaging, Biomaterials 29 (29) (2008) 4012–4021.
[8] R.D. Hergt, S. Dutz, Magnetic particle hyperthermia: biophysical limitations of a visionary tumour therapy, Journal of Magnetism and Magnetic Materials 311 (2007) 187–192.
[9] A. Jordan, R. Scholz, P. Wust, H. Fähling, R. Felix, Magnetic fluid hyperthermia (MFH): cancer treatment with AC magnetic field induced excitation of biocompatible superparamagnetic nanoparticles, Journal of Magnetism and Magnetic Materials 201 (1999) 413–419.
[10] D.A. Maity, D.C. Agrawal, Synthesis of iron oxide nanoparticles under oxidizing environment and their stabilization in aqueous and non-aqueous media, Journal of Magnetism and Magnetic Materials 308 (2007) 46–55.
[11] F.L. Mi, C.Y. Kuan, S.S. Shyu, S.T. Lee, S.F. Chang, The study of gelation kinetics and chain-relaxation properties of glutaraldehyde cross-linked chitosan gel and their effects on microspheres preparation and drug release, Carbohydrate Polymers 41 (2000) 389–396.
[12] K. Byrappa, S. Ohara, T. Adschiri, Nanoparticles synthesis using supercritical fluid technology-towards biomedical applications, Advanced Drug Delivery Reviews 60 (3) (2008) 299–327.
[13] X. Wei, R.C. Viadero Jr., Synthesis of magnetite nanoparticles with ferric iron recovered from acid mine drainage: implications for environmental engineering, Colloids and Surfaces A: Physicochemical and Engineering Aspects 294 (1–3) (2007) 280–286.
[14] G. Gnanaprakash, S. Mahadevan, T. Jayakumar, P. Kalyanasundaram, J. Philip, B. Raj, Effects of initial pH and temperature of iron salt solutions on formation of magnetite nanoparticles, Materials Chemistry and Physics 103 (2007) 168–175.
[15] C.H. Chia, S. Zakaria, R. Farahiyan, T.K. Liew, K.L. Nguyen, M. Abdullah, S. Ahmad, Size-controlled synthesis and characterization of Fe_3O_4 nanoparticles by chemical coprecipitation method, Sains Malaysiana 37 (4) (2008) 389–394.
[16] G.Y. Li, Y.R. Jiang, K.L. Huang, P. Ding, J. Chen, Preparation and properties of magnetic Fe_3O_4–chitosan nanoparticles, Journal of Alloys and Compounds 466 (1–2) (2008) 451–456.
[17] X. Wu, J.Y. Tang, Y.C. Zhang, H. Wang, Low temperature synthesis of Fe_3O_4 nanocrystals by hydrothermal decomposition of a metallorganic molecular precursor, Materials Science and Engineering B 157 (2009) 81–86.
[18] B. Mao, Z. Kang, E. Wang, S. Lian, L. Gao, C. Tian, C. Wang, Synthesis of magnetite octahedrons from iron powders through a mild hydrothermal method, Materials Research Bulletin 41 (2006) 2226–2231.
[19] K.C. Kim, E.K. Kim, J.W. Lee, S.L. Maeng, Y.S. Kim, Synthesis and characterization of magnetite nanopowders, Current Applied Physics 8 (2008) 758–760.
[20] J. Wang, M. Yao, G.J. Xu, P. Cui, J.T. Zhao, Synthesis of monodisperse nanocrystals of high crystallinity magnetite through solvothermal process, Materials Chemistry and Physics 3 (1) (2008) 6–9.
[21] I. Nedkov, S. Kolev, K. Zadro, K. Krezhov, T. Merodiiska, Crystalline anisotropy and cation distribution in nanosized quasi-spherical ferroxide particles, Journal of Magnetism and Magnetic Materials 272–276 (1) (2004) 1175–1176.
[22] J.Y. Park, E.S. Choi, M.J. Baek, G.H. Lee, Colloidal stability of amino acid coated magnetite nanoparticles in physiological fluid, Materials Letters 63 (2009) 379–381.
[23] L. Zhang, R. He, H.C. Gu, Oleic acid coating on the monodisperse magnetite nanoparticles, Applied Surface Science 253 (2006) 2611–2617.
[24] E.D. Piron, A. Domard, Interaction between chitosan and uranyl ions. Part 2. Mechanism of interaction, International Journal of Biological Macromolecules 22 (1998) 33–40.
[25] M. Ma, Y. Zhang, W. Yu, H.Y. Shen, H.Q. Zhang, N. Gu, Preparation and characterization of magnetite nanoparticles coated by amino silane, Colloids and Surfaces A: Physicochemical Engineering Aspects 212 (2003) 219–226.